

## Tetracyanoanthraquinodimethanes Having Biaryl Substituents: Synthesis, Crystal Structures, and Physical Properties

Hiroshi Chiba, Jun-ichi Nishida, and Yoshiro Yamashita\*

Department of Electronic Chemistry, Interdisciplinary Graduate School of Science and Engineering,  
Tokyo Institute of Technology, 4259 Nagatsuta, Midori-ku, Yokohama, Kanagawa 226-8502

(Received January 28, 2012; CL-120070; E-mail: yoshiro@echem.titech.ac.jp)

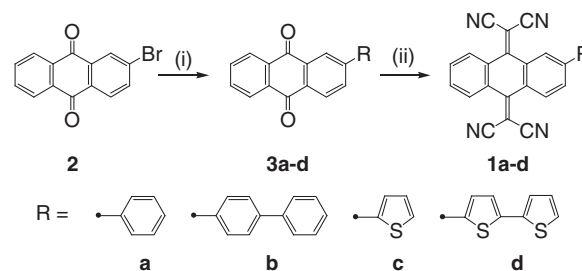
11,11,12,12-Tetracyano-9,10-anthraquinodimethane (TCNAQ) derivatives having four types of aryl substituents, phenyl, biphenyl-4-yl, thien-2-yl, and 2,2'-bithiophen-5-yl groups at their 2-position, were synthesized and characterized. Their crystal structures were determined by single-crystal X-ray structure analysis, revealing that the TCNAQ moiety and electron-donating substituents form donor-acceptor-segregated columnar structures. The combination of nonplanar electron acceptor TCNAQ and planar donor units provides a good way to afford segregated columnar structures.

Donor-acceptor-segregated columnar structures have attracted much attention since they afford good carrier transportation, and are advantageous for organic photovoltaics.<sup>1</sup> Oligothiophene-C<sub>60</sub> dyads<sup>2</sup> and  $\pi$ -extended sumanenes,<sup>3</sup> which consist of nonplanar acceptor units linked with planar aryl donor units, form donor-acceptor-segregated columnar stacks, suggesting that nonplanar electron acceptors with planar electron-donating substituents are promising compounds to afford such structures.

11,11,12,12-Tetracyano-9,10-anthraquinodimethane (TCNAQ)<sup>4</sup> is a dibenzo analogue of tetracyanoquinodimethane (TCNQ) and has a butterfly-shaped structure due to the steric interaction between the dicyanomethylene parts and the neighboring hydrogens.<sup>5</sup> The TCNAQ derivatives are expected to form donor-acceptor-segregated columnar structures by introducing planar electron donor units to the nonplanar electron acceptor moiety. We have now synthesized TCNAQs with four types of aryl substituents, phenyl (**1a**), biphenyl-4-yl (**1b**), thien-2-yl (**1c**), and 2,2'-bithiophen-5-yl (**1d**) groups at their 2-position, and investigated their crystal structures by single-crystal X-ray structure analysis. We report here the donor-acceptor-segregated columnar structures in the TCNAQs with biaryl substituents.

The synthesis of TCNAQs is outlined in Scheme 1. 2-Bromoanthraquinone (**2**) reacted with aryl boronic acids by the palladium-catalyzed Suzuki coupling reaction, or reacted with tributylstannyl reagents by the palladium-catalyzed Stille coupling to give the aryl-substituted derivatives.<sup>6,7</sup> TCNAQs **1a-1d** were obtained by a TiCl<sub>4</sub>-catalyzed Knoevenagel reaction with malononitrile.<sup>6,8</sup> They were characterized by mass spectrometry (MS) and <sup>1</sup>H NMR along with elemental analysis.

Cyclic voltammograms of TCNAQs **1a-1d** shown in Figure S5<sup>17</sup> were measured in CH<sub>2</sub>Cl<sub>2</sub> to investigate their electrochemical properties. The redox potentials are summarized in Table 1. All these compounds **1a-1d** showed a reversible reduction wave ascribed to two-electron reduction of the TCNAQ moiety.<sup>13</sup> The reduction potentials appeared at ca. -0.37 V vs. SCE and are almost the same among **1a-1d**. This suggests weak electronic interactions between the aryl substitu-



**Scheme 1.** Synthetic route to compounds **1a-1d**. (i) **3a** and **3b**: R-B(OH)<sub>2</sub>, [Pd(PPh<sub>3</sub>)<sub>4</sub>], K<sub>2</sub>CO<sub>3</sub>(aq), toluene, reflux; **3c** and **3d**: R-SnBu<sub>3</sub>, [Pd(PPh<sub>3</sub>)<sub>4</sub>], toluene, reflux; (ii) H<sub>2</sub>C(CN)<sub>2</sub>, TiCl<sub>4</sub>, pyridine, CH<sub>2</sub>Cl<sub>2</sub>, rt.

**Table 1.** Optical and electrochemical data of **1a-1d**<sup>9</sup>

| Compound  | $\lambda_{\text{abs}}/\text{nm}$ (log $\epsilon$ ) <sup>a</sup> | $E_{\text{pc}}^{\text{b}}$<br>/V | $E_{\text{pa}}^{\text{c}}$<br>/V |
|-----------|---|----------------------------------|----------------------------------|
| <b>1a</b> | 298 (4.44), 324 (4.47)  | -0.35                            |                                  |
| <b>1b</b> | 282 (4.54), 335 (4.58), 425 (3.98)                              | -0.36                            |                                  |
| <b>1c</b> | 288 (4.36), 343 (4.50), 442 (3.87)                              | -0.38                            |                                  |
| <b>1d</b> | 286 (4.35), 351 (4.58), 501 (4.02)                              | -0.38                            | +1.35                            |

<sup>a</sup>In CH<sub>2</sub>Cl<sub>2</sub>. <sup>b</sup>0.1 M *n*-Bu<sub>4</sub>NPF<sub>6</sub> in CH<sub>2</sub>Cl<sub>2</sub>, Pt electrode, V vs. SCE. <sup>c</sup>CV, irreversible wave, peak potential.

ents and TCNAQ moiety upon reduction.<sup>14</sup> TCNAQs **1a-1c** showed no oxidation waves, whereas **1d** showed an irreversible oxidation wave originating from the bithienyl units.

Their optical properties were investigated by the absorption spectra. Figure 1 shows the UV-vis absorptions of **1a-1d** in CH<sub>2</sub>Cl<sub>2</sub>. The absorption maxima of **1b**, **1c**, and **1d** in the visible region were observed at 425, 442, and 501 nm, respectively, which are attributed to charge transfer from the aryl donor substituents to the TCNAQ moiety.<sup>6</sup> Increasing the electron-donating properties of aryl substituents brings about more bathochromic shifts. The reflection spectra of **1a-1d** in the solid state were collected by using an integrated sphere and are depicted in Figure 2. Compared to the spectra in solution, the absorption edges reach longer wavelengths. This is due to the stronger intra- and intermolecular charge transfer in the solid state.

Their crystal structures were investigated by single-crystal X-ray structure analysis. Single crystals of **1a-1d** suitable for X-ray analysis were obtained by slow evaporation of the solvent from their CH<sub>2</sub>Cl<sub>2</sub>/hexane solution. Figure S1<sup>17</sup> shows the crystal structures of **1a** and **1c**. These two molecules form dimeric structures, and no interaction was observed between the aryl substituents. In the case of biphenyl-substituted derivative

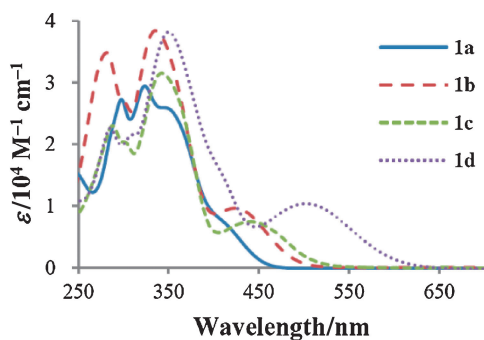


**Figure 1.** UV-vis absorption spectra of **1a–1d** in  $\text{CH}_2\text{Cl}_2$ .

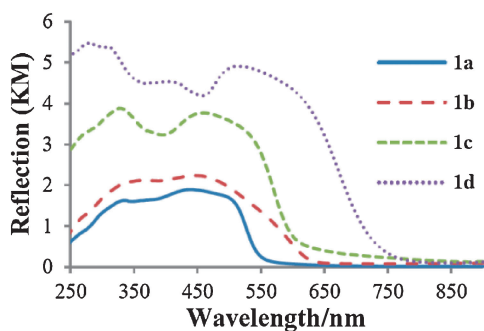


**Figure 2.** Reflection spectra of **1a–1d** in the solid state after K–M transformation.

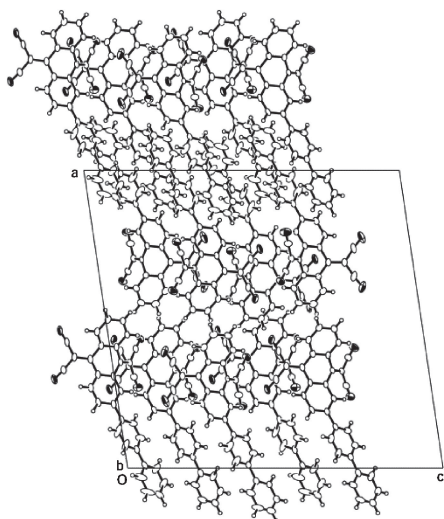


**Figure 3.** Crystal structure of **1b** viewed along the *b* axis.

**1b**, the solvent  $\text{CH}_2\text{Cl}_2$  molecules are included and interactions between the biphenyl units are observed (Figure S3<sup>17</sup>). The single crystals without the solvent molecules were obtained by slow sublimation. In the crystal of **1b**, the TCNAQ moieties assemble themselves, and a donor–acceptor-segregated columnar structure is constructed (Figure 3). In this case,  $\text{CH}\cdots\pi$  interactions are observed, and they seem to contribute to the formation of herringbone stacking of the biphenyl units. This remarkable change at the structure in **1b** compared to **1a** can be attributed to the extended  $\pi$  conjugation of the biphenyl group to give favorable intermolecular interactions.<sup>15</sup>

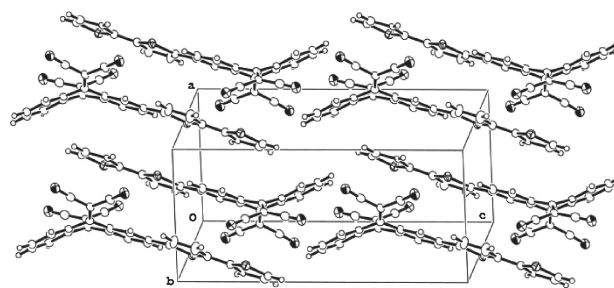


**Figure 4.** Crystal packing of **1d**.

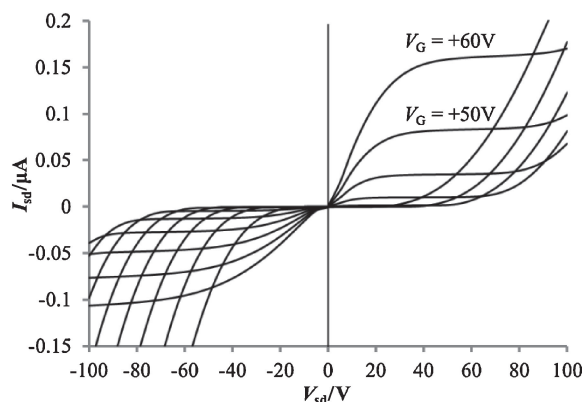


**Figure 5.** Ambipolar characteristic of **1d**.

Similar segregated stacking was observed in the crystal structure of 2,2'-bithiophen-5-yl-substituted derivative **1d** shown in Figure 4. In this case, effective  $\pi$ -stacking interaction can be seen between the bithienyl units, where the distance between these  $\pi$ -stacked units is 3.44 Å. This intermolecular interaction between the planar donor units seems to result in formation of a donor–acceptor-segregated columnar structure.

To investigate the relationship between the donor–acceptor-segregated structures and carrier-transport properties, field-effect transistor (FET) characteristics based on **1a–1d** were measured. The FET devices were fabricated with bottom-contact configuration. Thin films (500 Å) of compounds **1a–1d** were deposited on the channel regions kept at rt by vacuum evaporation. The measurements were carried out in situ under high vacuum ( $10^{-5}$  Pa). The films of **1b** and **1d** exhibited n-type semiconducting behavior. The electron mobilities (on/off ratio) were calculated to be  $6.6 \times 10^{-7} \text{ cm}^2 \text{ V}^{-1} \text{ s}^{-1}$  (800) for **1b** and  $3.4 \times 10^{-6} \text{ cm}^2 \text{ V}^{-1} \text{ s}^{-1}$  (1000) for **1d**.<sup>16</sup> In addition, an ambipolar characteristic of **1d** was observed due to the electron-donating bithienyl units (Figure 5). The hole mobility (on/off ratio) of **1d** was calculated to be  $3.6 \times 10^{-7} \text{ cm}^2 \text{ V}^{-1} \text{ s}^{-1}$  (1000). In contrast, **1c** showed no semiconducting behavior. This indicates that the donor–acceptor-segregated structure of **1d** is advantageous for carrier transport. Unfortunately, X-ray diffractograms of the films of **1a–1d** showed that the films were not completely crystalline.

In summary, TCNAQs bearing four types of aryl substituents **1a–1d** were synthesized, and their crystal structures were investigated by X-ray analysis. The derivatives with electron-donating biaryl substituents, **1b** and **1d** form donor–acceptor-segregated columnar structures. This is attributed to the

intermolecular interactions between donor units. The combination of nonplanar acceptor TCNAQ and extended  $\pi$ -conjugated planar donor units provides a good way to afford such segregated structures. The greater elongation of the  $\pi$  conjugation of donor units is thought to promote better carrier transportation, and study along this line is underway in our laboratory.

## References and Notes

- a) H. Hayashi, W. Nishihashi, T. Umeyama, Y. Matano, S. Seki, Y. Shimizu, H. Imahori, *J. Am. Chem. Soc.* **2011**, *133*, 10736. b) A. Kira, T. Umeyama, Y. Matano, K. Yoshida, S. Isoda, J. K. Park, D. Kim, H. Imahori, *J. Am. Chem. Soc.* **2009**, *131*, 3198.
- a) J. L. Segura, N. Martín, D. M. Guldi, *Chem. Soc. Rev.* **2005**, *34*, 31. b) W.-S. Li, Y. Yamamoto, T. Fukushima, A. Saeki, S. Seki, S. Tagawa, H. Masunaga, S. Sasaki, M. Takata, T. Aida, *J. Am. Chem. Soc.* **2008**, *130*, 8886.
- T. Amaya, K. Mori, H.-L. Wu, S. Ishida, J.-i. Nakamura, K. Murata, T. Hirao, *Chem. Commun.* **2007**, 1902.
- R. Gómez, C. Seoane, J. L. Segura, *Chem. Soc. Rev.* **2007**, *36*, 1305.
- a) C. Kabuto, Y. Fukazawa, T. Suzuki, Y. Yamashita, T. Miyashi, T. Mukai, *Tetrahedron Lett.* **1986**, *27*, 925. b) T. Suzuki, K. Ichioka, H. Higuchi, H. Kawai, K. Fujiwara, M. Ohkita, T. Tsuji, Y. Takahashi, *J. Org. Chem.* **2005**, *70*, 5592. c) K. Isoda, T. Yasuda, T. Kato, *J. Mater. Chem.* **2008**, *18*, 4522. d) M. Á. Herranz, B. Illescas, N. Martín, *J. Org. Chem.* **2000**, *65*, 5728. e) D. F. Perepichka, M. R. Bryce, A. S. Batsanov, J. A. K. Howard, A. O. Cuello, M. Gray, V. M. Rotello, *J. Org. Chem.* **2001**, *66*, 4517. f) T. Mukai, T. Suzuki, Y. Yamashita, *Bull. Chem. Soc. Jpn.* **1985**, *58*, 2433.
- F. Bureš, W. B. Schweizer, C. Boudon, J.-P. Gisselbrecht, M. Gross, F. Diederich, *Eur. J. Org. Chem.* **2008**, 994.
- M. Mamada, J.-i. Nishida, S. Tokito, Y. Yamashita, *Chem. Commun.* **2009**, 2177.
- a) B. S. Ong, B. Keoshkerian, *J. Org. Chem.* **1984**, *49*, 5002. b) W. Lehnert, *Tetrahedron Lett.* **1970**, *11*, 4723. c) W. Lehnert, *Synthesis* **1974**, 667.
- X-ray measurement of single crystals of **1a–1d** was carried out using a RAXIS-RAPID imaging plate diffractometer with MoK $\alpha$  radiation ( $\lambda = 0.71075$  Å) at  $-180.0$  °C. The structures were solved by the direct method (SIR2004<sup>10</sup>) and refined by the full-matrix least-squares method on  $F^2$ . The non-hydrogen atoms were refined anisotropically. Hydrogen atoms were refined using the riding model. Absorption correction was applied using an empirical procedure. All calculations were performed using the CrystalStructure crystallographic software package<sup>11</sup> except for refinement, which was performed using SHELXL-97.<sup>12</sup>  
*Crystal Data for 1a*: C<sub>26</sub>H<sub>12</sub>N<sub>4</sub>,  $M_r = 380.41$ , orange platelet, crystal dimensions  $0.79 \times 0.35 \times 0.08$  mm<sup>3</sup>, monoclinic, space group  $P2_1/c$ ,  $a = 10.5382(8)$  Å,  $b = 8.8850(6)$  Å,  $c = 20.5763(14)$  Å,  $\beta = 103.342(3)^\circ$ ,  $V = 1874.6(3)$  Å<sup>3</sup>,  $Z = 4$ ,  $D_{\text{calcd}} = 1.348$  g cm<sup>-3</sup>, 17841 reflections collected, 4290 independent ( $R_{\text{int}} = 0.0654$ ), GOF = 0.977,  $R_1 = 0.0505$  ( $I > 2.00\sigma(I)$ ),  $wR_2 = 0.1548$  for all reflections. *Crystal Data for 1b*: C<sub>32</sub>H<sub>16</sub>N<sub>4</sub>,  $M_r = 456.51$ , red block, crystal dimensions  $0.78 \times 0.60 \times 0.15$  mm<sup>3</sup>, monoclinic, space group  $P2_1/c$ ,  $a = 25.424(8)$  Å,  $b = 10.236(4)$  Å,  $c = 26.623(9)$  Å,  $\beta = 98.363(4)^\circ$ ,  $V = 6855(4)$  Å<sup>3</sup>,  $Z = 12$ ,  $D_{\text{calcd}} = 1.327$  g cm<sup>-3</sup>, 63117 reflections collected, 15636 independent ( $R_{\text{int}} = 0.0766$ ), GOF = 0.945,  $R_1 = 0.1423$  ( $I > 2.00\sigma(I)$ ),  $wR_2 = 0.3647$  for all reflections. *Crystal Data for 1c*: C<sub>24</sub>H<sub>10</sub>N<sub>4</sub>S,  $M_r = 386.43$ , red block, crystal dimensions  $0.79 \times 0.78 \times 0.30$  mm<sup>3</sup>, monoclinic, space group  $P2_1/n$ ,  $a = 10.6356(14)$  Å,  $b = 8.7879(10)$  Å,  $c = 20.671(3)$  Å,  $\beta = 105.652(4)^\circ$ ,  $V = 1860.4(4)$  Å<sup>3</sup>,  $Z = 4$ ,  $D_{\text{calcd}} = 1.380$  g cm<sup>-3</sup>, 16669 reflections that were collected, 4198 independent ( $R_{\text{int}} = 0.0744$ ), GOF = 1.027,  $R_1 = 0.0758$  ( $I > 2.00\sigma(I)$ ),  $wR_2 = 0.2472$  for all reflections. *Crystal Data for 1d*: C<sub>28</sub>H<sub>12</sub>N<sub>4</sub>S<sub>2</sub>,  $M_r = 468.55$ , dark platelet, crystal dimensions  $0.40 \times 0.40 \times 0.05$  mm<sup>3</sup>, triclinic, space group  $P\bar{1}$ ,  $a = 7.9373(14)$  Å,  $b = 8.5539(13)$  Å,  $c = 17.541(3)$  Å,  $\alpha = 95.943(5)^\circ$ ,  $\beta = 92.338(5)^\circ$ ,  $\gamma = 112.949(5)^\circ$ ,  $V = 1086.5(3)$  Å<sup>3</sup>,  $Z = 2$ ,  $D_{\text{calcd}} = 1.432$  g cm<sup>-3</sup>, 10508 reflections collected, 4947 independent ( $R_{\text{int}} = 0.0798$ ), GOF = 1.354,  $R_1 = 0.0931$  ( $I > 2.00\sigma(I)$ ),  $wR_2 = 0.2625$  for all reflections. The CCDC reference numbers are 867047–867051.
- SIR2004: M. C. Burla, R. Caliandro, M. Camalli, B. Carrozzini, G. L. Cascarano, L. De Caro, C. Giacovazzo, G. Polidori, R. J. Spagna, *J. Appl. Crystallogr.* **2005**, *38*, 381.
- CrystalStructure: Crystal Structure Analysis Package*, Rigaku and Rigaku/MSK, The Woodlands, TX 77381, USA, **2007**.
- G. M. Sheldrick, *SHELXL-97, Program for the Refinement of Crystal Structures*, University of Göttingen, Germany, **1997**.
- a) J. Santos, B. M. Illescas, N. Martín, J. Adrio, J. C. Carretero, R. Viruela, E. Ortí, F. Spänig, D. M. Guldi, *Chem.—Eur. J.* **2011**, *17*, 2957. b) R. Gómez, J. L. Segura, N. Martín, *Tetrahedron Lett.* **2006**, *47*, 6445. c) J. L. Segura, R. Gómez, R. Blanco, E. Reinold, P. Bäuerle, *Chem. Mater.* **2006**, *18*, 2834.
- a) N. Martín, I. Pérez, L. Sánchez, C. Seoane, *J. Org. Chem.* **1997**, *62*, 870. b) R. Gómez, J. L. Segura, N. Martín, *J. Org. Chem.* **2000**, *65*, 7566.
- T. Kojima, D. Kumaki, J.-i. Nishida, S. Tokito, Y. Yamashita, *J. Mater. Chem.* **2011**, *21*, 6607.
- The SiO<sub>2</sub> (300 nm) surface was treated with hexamethyldisilazane (HMDS) and kept rt. Threshold voltages were estimated at +52 V for **1b** and +31 V, -35 V for **1d**.
- Supporting Information is available electronically on the CSJ-Journal Web site, <http://www.csj.jp/journals/chem-lett/index.html>.